

Nuclear symmetry energy slope and its impact on exotic magnetized matter

Vivek Baruah Thapa¹, Debraj Kundu^{2,3} and Monika Sinha²

¹Department of Physics, Bhawanipur Anchalik College, Assam-781352, India

²Department of Physics, Indian Institute of Technology Jodhpur, Rajasthan-342030, India

³Department of Physics & Astronomy, University of Tennessee, Knoxville, TN 37996, USA

E-mail: vivek.thapa@bacollege.ac.in

Abstract. We explore the impact of the nuclear symmetry energy slope on the equation of state (EoS) for dense matter, considering exotic matter with Δ admixture in neutron stars. This investigation extends to its repercussions on observable properties of neutron stars, including mass-radius relationships and tidal responses. The EoS is formulated using the framework of covariant density functional theory. This formulation integrates density-dependent coupling schemes and accommodates the existence of non-nucleonic degrees of freedom in heavier systems. The adjustment of the symmetry energy parameter slope is determined by considering the density-dependent behavior of isovector meson coupling to baryons. Additionally, considering the substantial surface magnetic fields of compact stars, we examine the influence of strong magnetic fields on exotic matter. It is observed that strong magnetic fields impact (anti)kaons, causing a delay in their appearance and ultimately resulting in a stiffening of the EoS.

1. Introduction

Being one of the mysterious objects in the Universe and born from supernova explosion, a neutron star (NS) possesses matter densities of up to several times that of nuclear saturation (n_0). This makes these compact stars to be ideal laboratories to investigate extreme dense matter. Very recently, many astrophysical observations indicate the lower mass limit of these compact objects to be $\geq 2 M_\odot$ indicating the possibility of exotic matter existence in the core of NSs. The gravitational equilibrium within a NS is primarily sustained through the neutron degeneracy pressure, complemented by contributions from protons and leptons (specifically, electrons and muons). Furthermore, the exceedingly high matter density within NSs creates conditions conducive to the possible manifestation of exotic particles. Among these, hyperons, a distinct class of particles, may emerge within the NS if the baryon chemical potential attains a sufficiently elevated level. This particular inclusion of exotic particles in the dense matter was initially postulated in Ref.-[1]. Based on the same principle yet another class of particle entities, namely Δ -resonances, can be included in the particle spectrum of dense matter inside NSs as reported in Ref.-[2]. Additionally, it was reported in Ref.-[3] that due to the early onset of Δ -resonances, the hyperons are forced to appear at a later or higher density regimes. In a similar vein, an additional augmentation to the degrees of freedom may arise with the potential emergence of meson condensates [4], particularly when the lepton chemical potential attains elevated levels. While some works [5, 6] reveal that the condensation of π -mesons may not be possible in the interior of NS due to the repulsive $\pi - \pi$ potential derived from s-wave



Content from this work may be used under the terms of the [Creative Commons Attribution 4.0 licence](#). Any further distribution of this work must maintain attribution to the author(s) and the title of the work, journal citation and DOI.

πN scattering. Notwithstanding, some studies [7, 8] posit the pion condensation, given that the nature of the p -wave scattering potential is attractive. On the contrary, (anti)kaon could manifest as s-wave Bose condensates, given the attractive properties of the optical potential corresponding to (anti)kaons. The repulsive optical potentials of K^+ and K^0 kaons, however, result in an increase in their effective masses in nuclear matter, discouraging their presence in NS matter. Existence of the exotic degrees of freedom significantly affects the thresholds for the (anti)-kaon appearance in dense matter [9].

The symmetry energy (E_{sym}) plays a pivotal role in influencing the nucleonic energy density within nuclear matter. As such, the nuclear parameters associated with isospin dependence (*i.e.*) nuclear symmetry energy and its corresponding density dependence ($L_{\text{sym}} = \partial E_{\text{sym}} / \partial n$) play a pivotal role in understanding the dense matter behaviour [10, 11]. Concerning finite nuclei, the role of symmetry energy in determining the mass of the nuclei is considerably modest when contrasted with other components in the semi-empirical mass formula. Previous investigations [12, 13, 14] have been conducted to constrain the values of E_{sym} and L_{sym} at n_0 based on data from various astrophysical observations as well as terrestrial experiments. The estimated values of $E_{\text{sym}}(n_0)$ and $L_{\text{sym}}(n_0)$ fall within the ranges of 28.5 – 34.9 MeV and 30.6 – 86.8 MeV, respectively, as reported in various models [15].

An inherent characteristic of NSs lies in their robust surface magnetic fields, spanning the range of 10^8 to 10^{16} Gauss (G). A distinct subgroup of NSs, identified as magnetars, exhibits an exceptionally intense surface magnetic field, typically falling within the range of 10^{14} to 10^{16} G [16, 17]. In our current investigation, we initially delineate the constraints on model coupling sets from observational constraints, including measurements related to NS structure of numerous pulsars and matter deformability assessments from gravitational wave (GW) measurement constraints. Subsequently, employing the model constrained from the observational measurements, we examine the characteristics of exotic dense matter and NSs characterized by strong magnetic fields.

In the upcoming section (Section-2), the influence of extreme magnetic field on the exotic dense matter in interest will be explored. Following that, in Section-3, we will provide a discussion of the results obtained, with parameters associated with our dense matter model aligned with astrophysical observations.

2. Formalism

2.1. Dense Matter Model

This paper presents a novel exploration of the composition of matter within NSs, specifically those with strong magnetic fields, commonly known as magnetars. Our investigation incorporates various heavy exotic particles including the baryon octet, (anti)-kaons and nucleonic resonances in β -equilibrium. The interactions between particles are described using the covariant density functional (CDF) model. In this study, we employ the density-dependent CDF (DD-CDF) model to analyze the impact of a strong magnetic field on exotic dense matter interior to the compact objects. This model describes the strong forces between nucleons, hyperons, (anti)kaons, and Δ -resonances using specific meson fields. The isoscalar-scalar σ , isoscalar-vector ω_μ , and isovector-vector ρ_μ fields play a key role in mediating these interactions. Furthermore, the strange isoscalar-vector meson field ϕ_μ is included to account for interactions specifically between hyperons and between hyperons and (anti)kaons. By incorporating the effects of these interactions, the RMF model provides insights into the equation of state of neutron star matter, which is crucial for understanding their structure, stability, and various astrophysical phenomena.

The system's Lagrangian density is provided by the sum of Lagrangian densities of the dense matter and the electro-magnetic fields [18]. The magnetic field is oriented along the z -axis, with $A^\mu \equiv (0, -yB, 0, 0)$ representing its four-vector potential. Because of the magnetic field, the

particles possessing electric charges experience Landau quantization resulting in their respective motions perpendicular to the direction of the existing magnetic field. $p_{\perp} = 2\nu e|Q|B$ gives the momentum in the perpendicular direction to the field direction where ν represents the Landau level. In case of particles governed by Dirac fields, the lowest Landau level possess a degeneracy of 1, while it is 2 for all other Landau levels [19]. For the Δ -baryons governed by the Schwinger-Rarita fields, the lowest level degeneracy is 2, followed by 3 for the next (second) level, and subsequently 4 in case of the remaining Landau levels [20]. Following the threshold conditions for the various exotic degrees of freedom, the equation of state, $P(\varepsilon)$ of the dense matter is then obtained following the additional constraints of neutrality of electric charges and conservation of baryon number in the dense matter of interest. The energy density of the dense nuclear matter is given by,

$$\varepsilon = \sum_b \varepsilon_b + \sum_{\Delta} \varepsilon_{\Delta} + \sum_l \varepsilon_l + \frac{1}{2} m_{\sigma}^2 \sigma^2 + \frac{1}{2} m_{\omega}^2 \omega_0^2 + \frac{1}{2} m_{\rho}^2 \rho_{03}^2 + \frac{1}{2} m_{\phi}^2 \phi_0^2 + m_K^* (n_{K^-} + n_{\bar{K}^0}) \quad (1)$$

where, ε_i with $i = b, \Delta, l$ represent the energy densities of baryon octet, Δ -baryons and leptons respectively. $n_{K^-}, n_{\bar{K}^0}$ depict the vector number densities of (anti)kaons in dense nuclear matter. The matter pressure is then subsequently evaluated by the Gibbs-Duhem relation. The matter pressure is not explicitly contributed to by (anti)kaons, as they exist as condensates of s-wave.

2.2. Coupling constants

In this work, we implement the DD scheme of couplings considering DD-ME2 [21] and DD-MEX [22] parametrization sets. In our calculations for the scalar meson-hyperon coupling constants, we adopt the optical potentials of Λ , Ξ , and Σ as follows: $U_{\Lambda} = -30$ MeV, $U_{\Xi} = -14$ MeV, and $U_{\Sigma} = +30$ MeV [23]. It is noteworthy to mention that because of the antagonistic tendency of Σ hyperons in dense matter, they do not manifest within the density range considered in our investigation. For the vector couplings (density-dependent) involving vector mesons and hyperons, we utilize SU(6) symmetry [24].

Since very sparse knowledge is available, we consider the Δ -coupling to scalar mesons as $R_{\sigma\Delta} = g_{\sigma\Delta}/g_{\sigma N} = 1.16$, adapted from Ref.-[23]. The vector couplings in the non-strange Δ -baryonic sector are specified as [25]: $g_{\omega\Delta} = 1.1g_{\omega N}$, $g_{\rho\Delta} = g_{\rho N}$. Due to absence of strangeness in Δ -baryons, we set $g_{\phi\Delta} = 0$.

The methodology to calculate the coupling values associated with the scalar meson with (anti)-kaons is elucidated in [26]. Various studies [27, 28, 29, 30, 31] have presented the K^- optical potential ($U_{\bar{K}}$) within the range of $-200 \leq U_{\bar{K}} \leq -40$ MeV. In our investigation, we adopt $U_{\bar{K}} = -130$ MeV. This $U_{\bar{K}}$ consideration is motivated by the results reported in Ref.-[2] which attempts to constrain the (anti)kaon optical potential in dense matter based on various neutron star astrophysical observables. The vector couplings (density-independent) associated with the (anti)kaons interaction with mesons are determined by the relations:

$$g_{\omega K} = \frac{1}{3} g_{\omega N}, \quad g_{\rho K} = g_{\rho N}, \quad g_{\phi K} = 4.27 \quad (2)$$

It is noteworthy that recent investigations viz. PREX and PREX-II suggest estimations on the nuclear parameters associated with isospin dependence as: symmetry energy, $E_{sym} = (38.1 \pm 4.7)$ MeV and its corresponding slope as, $L_{sym} = (106 \pm 37)$ MeV [32]. Based on the PREX-II estimations of isospin dependence nuclear parameters, their corresponding isovector coupling are adopted from Ref.-[33]. Due to the inconsistency with observational constraints, *i.e.* reduction of maximum mass of NS family, for these values of L_{sym} , E_{sym} , we consider them to be 70 MeV and 38.1 MeV, respectively and refrain from further consideration of them in the subsequent discussions in this paper.

2.3. Configuration of magnetic field in the compact stars

To investigate the influence of intense magnetic fields in dense matter with exotic degrees of freedom, we take into account the magnetic field profile derived in Ref.-[34]. This magnetic field profile is obtained by solving the fields equations introduced by Einstein and Maxwell and implementing a quadratic fit to it. This fitting is grounded on the assumption of a poloidal magnetic field and employs EoSs derived from different dense nuclear matter models. The specifics of this profile can be found in Ref.-[34, 35]. The expression for this profile is provided as follows: and the expression is given by,

$$B(\mu_B) = \frac{(a + b\mu_B + c\mu_B^2)}{B_c} \mu. \quad (3)$$

In the provided context, μ_B stands for the chemical potential of baryons, and μ represents the dipole magnetic moment of the NS. To ensure consistent units, μ_B and μ are measured in MeV and Am^2 , respectively. $B(\mu_B)$ is expressed in units of G. In case of electrons, the critical field is denoted as B_c , which corresponds to 4.414×10^{13} G. The considered values of the coefficients associated with the magnetic field profile fit (eqn.-3) are taken from Ref.-[18] and the interested readers may look into it for further clarification.

In our analysis, we consider two different magnitudes for the dipole magnetic moment: $\mu = 2 \times 10^{31} \text{ Am}^2$ and $\mu = 1.5 \times 10^{32} \text{ Am}^2$. These values correspond to central magnetic field strengths of roughly 1.2×10^{17} and 0.9×10^{18} G, respectively. Additionally, the surface magnetic field intensities for these instances are approximately 2.5×10^{16} G and 2×10^{17} G, respectively.

3. Results & Discussions

3.1. NS Structure Solutions

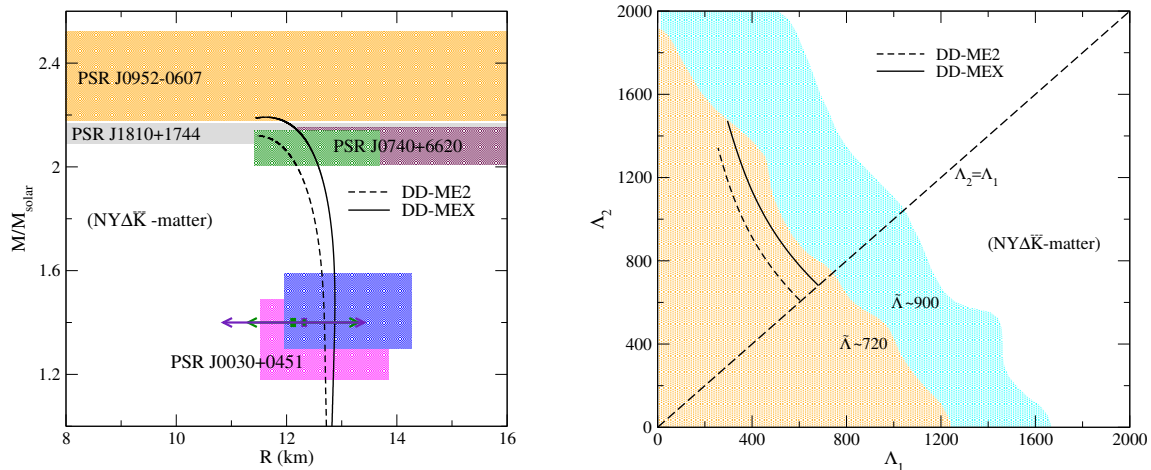


Figure 1. *Left panel:* NS structure solutions for the matter composition $N\bar{K}Y\Delta$ considering the coupling sets DD-ME2 and DD-MEX. The shaded regions in the plot represent observational constraints derived from various pulsars. The horizontal lines denote joint radius constraints derived from mass-radius estimation and GW event data for a canonical NS [36, 37]. *Right panel:* Tidal deformabilities Λ_1 and Λ_2 within the context of the matter composition $N\bar{K}Y\Delta$. The chirp mass is held constant at $\mathcal{M} = 1.188M_\odot$. The numerical values assigned to Λ_1 and Λ_2 correspond to the two masses M_1 and M_2 involved in GW170817 event. The highlighted areas in the graph depict the upper limits at a 90% confidence level for $\tilde{\Lambda} \sim 900$ (TaylorF2) and $\tilde{\Lambda} \sim 720$ (PhenomPNRT), as documented in [38, 39].

Examining the NS structure without considering the magnetic field effect, we investigate the mass-radius relationship based on the parametrizations DD-MEX and DD-ME2, as illustrated in the left panel of Fig. 1. The depicted figure shows that NSs composed of exotic dense matter, conform to astrophysical constraints regarding the mass-radius relationship for the considered coupling sets in this work. Although the DD-ME2 parametrization does not completely match the most recent observation of PSR J0952-0607, it is retained due to its alignment with all other observational constraints. Furthermore, both of these parametrizations adhere to the boundations on tidal deformability parameter derived from GW event data, as illustrated in the right panel of Fig. 1. Hence, in our investigation of the magnetic field's influence on NSs composed of matter containing baryon octet, (anti)kaon condensates as well as heavier nucleon resonances, we opt for the aforementioned coupling sets due to their consistency with astrophysical observations.

3.2. Particle population

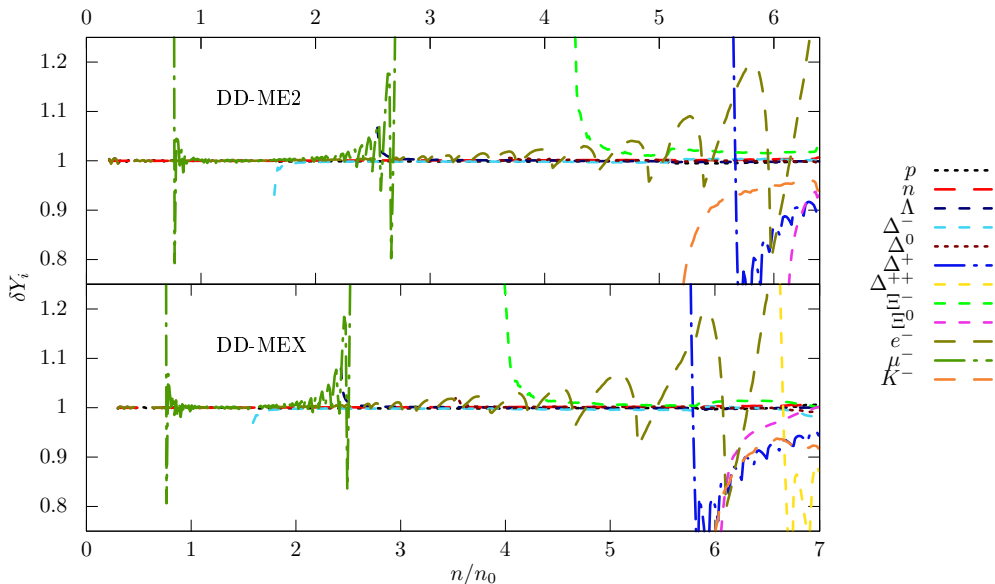


Figure 2. The modification of $\delta Y_i \equiv n_i(B)/n_i(0)$, is depicted varying with the total number density for a NS possessing a dipole moment of $\mu = 2 \times 10^{31} \text{ Am}^2$. DD-ME2 (upper panel) and DD-MEX (lower panel) coupling sets.

Fig. 2 illustrates how the magnetic field influences particle population, showcasing the ratio of particle density with a magnetic field ($n_i(B)$) to that without a magnetic field ($n_i(0)$) as a function of n/n_0 . The oscillations of the particle populations is due to the Landau quantization of the charged particles. The electrically uncharged particles are affected via the condition of conservation of baryon number in the dense matter system. It is observed from the figure that the occupation of Landau levels become more pronounced for the less massive particles at higher densities. This is because the magnetic field strength increases from the surface to the core of the compact star making the particles to behave highly quantized in nature.

Electrons, being lighter particles, exhibit more noticeable oscillations in their respective particle profile, especially at lower matter densities. For muons, initial oscillations result from their lower population density, leading to a smaller Fermi momentum and fewer maximum Landau levels, thus emphasizing Landau quantization.

For the case with magnetic field profile strength corresponding to $\mu = 2 \times 10^{31} \text{ Am}^2$, it is seen that the strength of magnetic field is close to 10^{16} G upto a matter density range of $2 n_0$. At this strength, protons experience minimal effects, and electrons exhibit little influence due to the magnetic field. Consequently, the proton population is only marginally impacted, and electrons occupy fewer Landau levels as the field strength approaches about 10^{17} G near a density of approximately $\sim 5 n_0$. This results in an increased electron fraction, causing a delay in the appearance of K^- and yielding $\delta Y_i < 1$ for K^- in subsequent densities. As a result, the densities at which the heavier particles such as Δ^+ , Ξ^0 , and Δ^{++} appear experience changes, and their existences in dense matter are shaped by the interplay of conservation of baryon number and the neutrality condition for electric charge.

In case of the magnetic moment strength of $\mu = 1.5 \times 10^{32} \text{ Am}^2$, a similar pattern is observed but with higher Landau quantization due to the high value of magnetic fields at early matter densities with the specified μ value.

3.3. Dirac Effective Mass of Nucleons

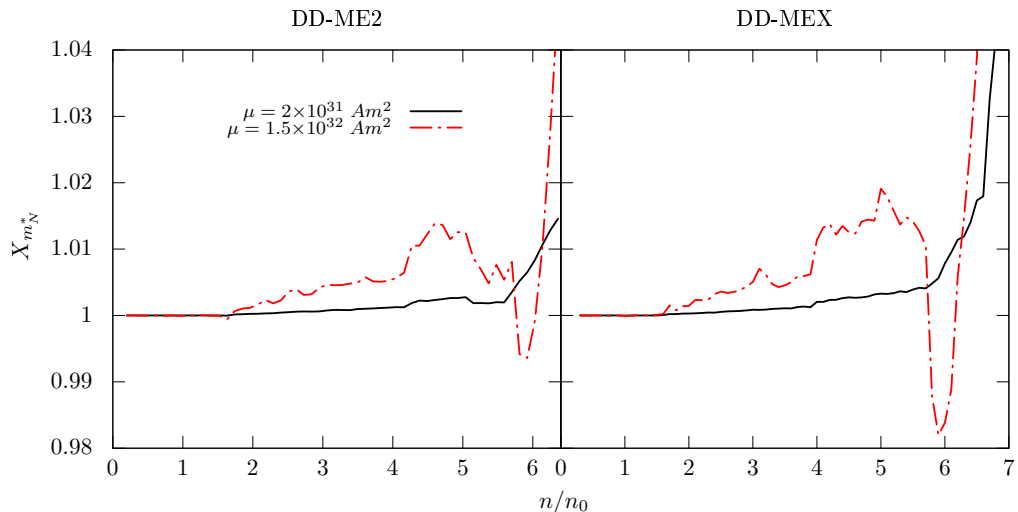


Figure 3. Graphs illustrating the ratio of the effective nucleonic Dirac mass with and without a magnetic field, are presented as functions of the total number density normalized to n_0 (n/n_0). The plots consider neutron star dipole moments of $\mu = 2 \times 10^{31} \text{ Am}^2$ and $\mu = 1.5 \times 10^{32} \text{ Am}^2$. The matter composition includes nucleons, antikaons, hyperons, and delta particles, and the parametrizations considered are DD-ME2 (left panel) and DD-MEX (right panel).

In Fig. 3, we present the change in the Dirac effective mass for nucleons with respect to n/n_0 in the cases with and with the influence of intense magnetic fields. Notably, distinct features become apparent in the figures, with the emergence of Δ^- evident around a density of approximately $\sim 1.6 n_0$. This oscillatory pattern is again associated with the quantization of Landau levels by the electrically charged particles, which, in turn, impacts various material properties such as mean-free path of baryons, specific heat, and thermal conductivity, among others. Examining these properties in-depth goes beyond the scope of the current study and will be addressed in future research.

4. Summary

Recent observations suggest that massive neutron stars may contain cores with densities above $2n_0$, potentially leading to the emergence of exotic matter, including strange baryons, kaons,

and strange quark matter (SQM). This study explores the effects of strong magnetic fields on dense neutron star matter, considering all possible exotic states like hyperons, Δ -resonances, and (anti)kaon condensates, particularly in the context of magnetars, which have extremely strong surface magnetic fields (ranging from $10^{13} - 10^{16}$ G). The internal magnetic field strength, though not directly observable, can be estimated through the Einstein-Maxwell field equations. We adopt a model where the magnetic field increases towards the star's center, being about an order of magnitude stronger at the core compared to the surface. Our findings indicate that (anti)kaon condensates appear at higher densities than the threshold for SQM, making them unlikely in hybrid star configurations. Using the DD-RMF model with DD-ME2 and DD-MEX parameter sets, we find that the magnetic field raises the density threshold for K^- formation, resulting in stiffer matter and a higher maximum mass for the star, with the effect being more pronounced in the DD-ME2 case.

This work is limited by its reliance on theoretical magnetic field models and specific parameter sets (DD-ME2 and DD-MEX) within the DD-RMF framework. Additionally, it does not explore the potential interplay between (anti)kaon condensates and SQM in hybrid star configurations, which requires further investigation.

Acknowledgments

The authors appreciate the constructive feedback provided by the anonymous referee, which significantly improved the quality of the manuscript.

References

- [1] Ambartsumyan V A and Saakyan G S 1960 *Sov. Astron.* **4** 187
- [2] Thapa V B, Sinha M, Li J J and Sedrakian A 2021 *Phys. Rev. D* **103**(6) 063004 URL <https://link.aps.org/doi/10.1103/PhysRevD.103.063004>
- [3] Thapa V B and Sinha M 2022 *Phys. Rev. C* **105**(1) 015802 URL <https://link.aps.org/doi/10.1103/PhysRevC.105.015802>
- [4] Pethick C J, Schaefer T and Schwenk A 2015 *arXiv e-prints* arXiv:1507.05839 (*Preprint* 1507.05839)
- [5] Glendenning N K 1985 *Astro. Phys. J.* **293** 470–493
- [6] Ohnishi A, Jido D, Sekihara T and Tsubakihara K 2009 *Phys. Rev. C* **80**(3) 038202 URL <https://link.aps.org/doi/10.1103/PhysRevC.80.038202>
- [7] Ericson T E O and Weise W 1988 *Pions and Nuclei* (Oxford, UK: Clarendon Press) ISBN 978-0-19-852008-5
- [8] Khunjua T, Klimenko K and Zhokhov R 2019 *Symmetry* **11** 778 (*Preprint* 1912.08635)
- [9] Char P and Banik S 2014 *Phys. Rev. C* **90**(1) 015801 URL <https://link.aps.org/doi/10.1103/PhysRevC.90.015801>
- [10] Ducoin C, Margueron J and Providência C 2010 *EPL (Europhysics Letters)* **91** 32001 (*Preprint* 1004.5197)
- [11] Lattimer J M and Prakash M 2016 *Phys. Rep.* **621** 127–164 (*Preprint* 1512.07820)
- [12] Lattimer J M and Steiner A W 2014 *European Physical Journal A* **50** 40 (*Preprint* 1403.1186)
- [13] Roca-Maza X, Viñas X, Centelles M, Agrawal B K, Colò G, Paar N, Piekarowicz J and Vretenar D 2015 *Phys. Rev. C* **92** 064304 (*Preprint* 1510.01874)
- [14] Tews I, Lattimer J M, Ohnishi A and Kolomeitsev E E 2017 *Astro. Phys. J.* **848** 105 (*Preprint* 1611.07133)
- [15] Oertel M, Hempel M, Klähn T and Typel S 2017 *Reviews of Modern Physics* **89** 015007 (*Preprint* 1610.03361)
- [16] Harding A K and Lai D 2006 *Reports on Progress in Physics* **69** 2631–2708 URL <https://doi.org/10.1088/0034-4885/69/9/r03>
- [17] Turolla R, Zane S and Watts A L 2015 *Reports on Progress in Physics* **78** 116901 URL <https://doi.org/10.1088/0034-4885/78/11/116901>
- [18] Kundu D, Thapa V B and Sinha M 2023 *Phys. Rev. C* **107**(3) 035807 URL <https://link.aps.org/doi/10.1103/PhysRevC.107.035807>
- [19] Sinha M, Mukhopadhyay B and Sedrakian A 2013 *Nuc. Phys. A* **898** 43–58 (*Preprint* 1005.4995)
- [20] de Paoli M G, Castro L B, Menezes D P and Barros C C J 2013 *Journal of Physics G Nuclear Physics* **40** 055007 (*Preprint* 1207.4063)
- [21] Lalazissis G A, Nikšić T, Vretenar D and Ring P 2005 *Phys. Rev. C* **71**(2) 024312 URL <https://link.aps.org/doi/10.1103/PhysRevC.71.024312>
- [22] Taninah A, Agbemava S, Afanasjev A and Ring P 2020 *Physics Letters B* **800** 135065 ISSN 0370-2693 URL <https://www.sciencedirect.com/science/article/pii/S0370269319307877>

[23] Thapa V B, Sinha M, Li J J and Sedrakian A 2020 *Particles* **3** 660–675 ISSN 2571-712X URL <https://www.mdpi.com/2571-712X/3/4/43>

[24] Hofmann F, Keil C M and Lenske H 2001 *Phys. Rev. C* **64**(2) 025804 URL <https://link.aps.org/doi/10.1103/PhysRevC.64.025804>

[25] Li J J and Sedrakian A 2019 *Phys. Rev. C* **100**(1) 015809 URL <https://link.aps.org/doi/10.1103/PhysRevC.100.015809>

[26] Thapa V B and Sinha M 2020 *Phys. Rev. D* **102**(12) 123007 URL <https://link.aps.org/doi/10.1103/PhysRevD.102.123007>

[27] Waas T and Weise W 1997 *Nuclear Physics A* **625** 287–306 ISSN 0375-9474 URL <https://www.sciencedirect.com/science/article/pii/S0375947497004879>

[28] Friedman E, Gal A, Mareš J and Cieplý A 1999 *Phys. Rev. C* **60**(2) 024314 URL <https://link.aps.org/doi/10.1103/PhysRevC.60.024314>

[29] Koch V 1994 *Physics Letters B* **337** 7–13 ISSN 0370-2693 URL <https://www.sciencedirect.com/science/article/pii/0370269394914346>

[30] Lutz M 1998 *Physics Letters B* **426** 12–20 ISSN 0370-2693 URL <https://www.sciencedirect.com/science/article/pii/S0370269398002998>

[31] Schaffner-Bielich J, Koch V and Effenberger M 2000 *Nuclear Physics A* **669** 153–172 ISSN 0375-9474 URL <https://www.sciencedirect.com/science/article/pii/S0375947499006909>

[32] Reed B T, Fattoyev F J, Horowitz C J and Piekarewicz J 2021 *Phys. Rev. Lett.* **126**(17) 172503 URL <https://link.aps.org/doi/10.1103/PhysRevLett.126.172503>

[33] Baruah Thapa V and Sinha M 2022 *arXiv e-prints* arXiv:2203.02272 (Preprint 2203.02272)

[34] Dexheimer V, Franzon B, Gomes R, Farias R, Avancini S and Schramm S 2017 *Physics Letters B* **773** 487–491 ISSN 0370-2693 URL <https://www.sciencedirect.com/science/article/pii/S0370269317307062>

[35] Rather I A, Rahaman U, Dexheimer V, Usmani A and Patra S 2021 *arXiv preprint arXiv:2104.05950*

[36] Jiang J L, Tang S P, Wang Y Z, Fan Y Z and Wei D M 2020 *The Astrophysical Journal* **892** 55 URL <https://doi.org/10.3847/1538-4357/ab77cf>

[37] Landry P, Essick R and Chatzioannou K 2020 *Phys. Rev. D* **101** 123007 (Preprint 2003.04880)

[38] Abbott B P, Abbott R *et al.* 2017 *Phys. Rev. Lett.* **119** 161101 (Preprint 1710.05832)

[39] Abbott B P, Abbott R *et al.* (LIGO Scientific Collaboration and Virgo Collaboration) 2019 *Phys. Rev. X* **9**(1) 011001 URL <https://link.aps.org/doi/10.1103/PhysRevX.9.011001>